# Electronic Supplementary Information

# CTAB-capped Mn-doped ZnS quantum dots and label-free aptamer for room-temperature phosphorescence detection of mercury ions

Wan Yi Xie, Wei Tao Huang, Hong Qun Luo*, and Nian Bing Li*

Key Laboratory of Eco-environments in Three Gorges Reservoir Region (Ministry of Education), School of Chemistry and Chemical Engineering, Southwest University, Chongqing 400715, P.R. China

* Corresponding authors: luohq@swu.edu.cn (H.Q. Luo)； linb@swu.edu.cn (N.B. Li)

# 1. Experimental Section

## Reagents and Apparatus

The oligonucleotide (T20: 5'- TTT TTT TTT TTT TTT TTT TT-3'; A20: 5'-AAA AAA AAA AAA AAA AAA AA-3'; DNA1: 5'-CTC TCT CTC TCT CTC TCT CTC-3'; DNA2: 5'-GAG AGA GAG AGA GAG AGA GAG-3') was prepared by Sangon Biotechnology Co., Ltd. (Shanghai, China). Single-stranded DNA concentrations were determined by measuring the absorbance at 260 nm. All reagents used were of analytical reagent grade. $ZnSO_4 \cdot 7H_2O$, $Mn(Ac)_2 \cdot 2H_2O$, $Na_2S \cdot 9H_2O$, L-cysteine (L-Cys), cetyltrimethylammonium bromide (CTAB), and 4-(2-hydroxyethyl)-1-piperazineethanesulfonic acid (HEPES) were purchased from Aladdin Ltd. (Shanghai, China). The used metal salts, i.e. $AgNO_3$, $BaCl_2$, $Cd(NO_3)_2$, $CoCl_2$, $CrCl_3$, $Cu(NO_3)_2$, $FeCl_3$, $Hg(NO_3)_2$, $Mn(Ac)_2$, $NaNO_3$, $Ni(NO_3)_2$, $Pb(NO_3)_2$, and $ZnCl_2$ were used as received without further purification. Stock solution of 5 μM T20 probe was prepared in HEPES buffer solution (10 mM, pH 7.4, 200 mM $NaNO_3$), and different concentrations of $Hg^{2+}$ were prepared in 10 mM HEPES buffer solution (pH 7.4).

The phosphorescence and fluorescence measurements were performed on an F-4500 spectrofluorophotometer (Hitachi, Japan) equipped with a xenon lamp excitation source. Ultraviolet-visible absorption spectra were recorded on a Shimadzu UV-2450 spectrophotometer (Suzhou Shimadzu Instrument Co., Ltd., China). Transmission electron microscopy (TEM) images were obtained with a transmission electron microscope (JEM-100CXII, Japan) at 80 KV accelerating voltage. The samples for TEM characterization were prepared by placing a drop of colloidal solution on carbon-coated copper grid and dried at room temperature. XRD patterns of L-Cys modified Mn-ZnS QDs were performed using an X-ray diffractometer (XRD) (Beijing Purkinje General Instrument Co., Ltd., China). Several relatively strong reflection peaks in the 2θ region of 10–80° were collected. pH values were measured by a pH-3C precision pH meter (Leici Devices Factory of Shanghai, China).

**Synthesis of the Mn-ZnS QDs**

Briefly, L-Cys (50.0 mL, 0.02 M), $ZnSO_4$ (5.0 mL, 0.1 M), and $Mn(Ac)_2$ (1.5 mL, 0.01M) were added to a three-necked flask. The mixed solution was adjusted to pH 11 with 1 M NaOH and stirred under argon for 30 min at room temperature. $Na_2S$ (5.0 mL, 0.1 M) was then rapidly added to the solution. The mixture was stirred for another 20 min, and followed by 2 h of aging at 50°C under air to form L-Cys-capped Mn-ZnS QDs. Finally, the prepared solution was filtered through a 0.22 μm membrane filter. For purification, the QDs were precipitated with ethanol and separated by centrifuging, and the residue was redissolved in water.

**$Hg^{2+}$ detection**

The protocol of our method is displayed in Scheme 1. Typically, 75 μL of the above L-Cys-capped Mn-ZnS QDs (1 mg/mL) colloidal solution was added to 380 μL of the HEPES (10 mM, pH 7.4) buffer solution, followed by the addition of 25 μL of CTAB (0.1 mM). The mixture was thoroughly mixed, and the CTAB/Mn-ZnS QDs were formed. For $Hg^{2+}$ detection, 10 μL of the 5 μM T20 probe solution and 10 μL of metal ion solution (or blank buffer solution) were mixed and incubated for ~0.5 h at room temperature, and double-stranded DNA (dsDNA) was formed by T-$Hg^{2+}$-T coordination chemistry. Then this formed dsDNA was added to the CTAB/Mn-ZnS QDs mixture. The solution was 500 μL in summation and was vortexed thoroughly. On excitation at 316 nm, the room temperature phosphorescence spectra of the mixture were measured in the region of 400 to 700 nm, and the intensities were detected at 595 nm with all excitation and emission slit widths of 10 nm. The working voltage of the PMT was 700 V. Meanwhile, the fluorescence spectra were recorded in the region of 400 to 700 nm on excitation at 316 nm, and all excitation and emission slit widths of 10 nm. The working voltage of the PMT was 400 V. For the RLS measurements, the fluorescence spectrophotometer was set in the synchronous mode with the slit widths of 5 and 5 nm for excitation and emission. The PMT voltage was set at 400 V.

## 2. Characterization of Mn-ZnS QDs

Figure S1A shows the X-ray powder diffraction (XRD) patterns for L-Cys-capped Mn-ZnS QDs. From this figure, it is shown that the powder exhibited a cubic zinc blende structure with peaks for (111), (220), and (311). The TEM image was also taken to characterize the product in our work. From the TEM image (Figure S1B), the size of the nanomaterials was 10-20 nm larger than the previous reports [1], which was mainly caused by soft reunion. The UV-vis absorption spectrum (curve *a*) and phosphorescence emission spectrum (curve *b*) are shown in Figure S1C. The observed phosphorescence can be attributed to the transition of $^4T_1$–$^6A_1$ d–d transition of $Mn^{2+}$ ions on $Zn^{2+}$ sites of the QDs. Mn-ZnS QDs display bright orange fluorescence in a UV lamp box (Figure S1D), suggesting a relatively high quantum yield of $Mn^{2+}$ transition emission.

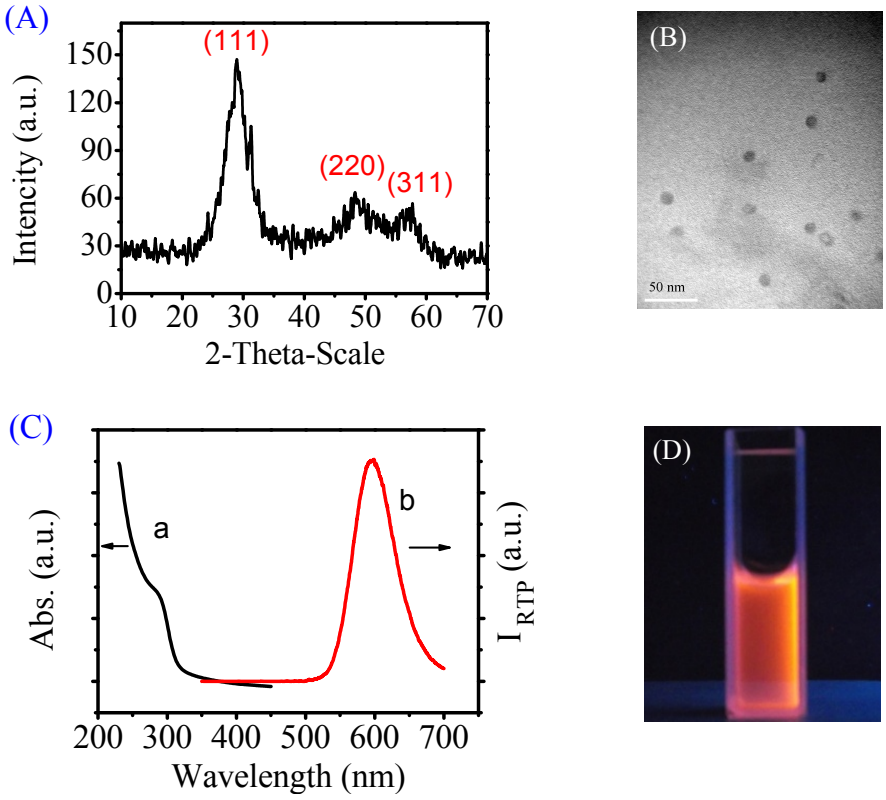


**Figure S1** Characterization of the L-Cys-capped Mn-ZnS QDs: (A) XRD pattern, (B) TEM image, (C) UV-vis absorption spectrum (curve *a*) and phosphorescence emission spectrum (curve *b*), (D) the photograph in a UV lamp box.

## 3. Dependent factors of interaction

Figure S2A shows that the concentration of CTAB affects the response behavior of the system for $Hg^{2+}$. In a neutral buffer solution, as the amount of CTAB increases, the QDs would tend to bind each other, which would finally lead to quench the RTP of the QDs. Thus too much CTAB would result in decrease in sensitivity of the proposed sensor. Considering the sensitivity in this study, 5 μM CTAB was selected as the optimum condition. Figure S2B illustrates the evaluation of pH effect. It was performed by dissolving the nanoparticles in different buffers with pH values from 5.7 to 12.0. This result shows that the phosphorescence quenching of Mn-ZnS QDs varied with the change in pH of the aqueous solution. The maximum change of RTP intensities appeared in the range of pH 7.2 to 7.9. In this study, the acidity of the aqueous medium was controlled by using HEPES buffer with pH 7.4. The amount of T20 also affects the sensitivity of our analytical system. Figure S2C illustrates the change in RTP of CTAB/Mn-ZnS upon addition of different concentrations of T20. As a result, the mixture containing 100 nM T20 was the optimum choice for this experiment. The effect of ionic strength on the assay was also investigated by adding $NaNO_3$ to the system. With increasing $NaNO_3$ concentration, the QDs aggregated and the emission of QDs was quenched (Figure S2D). On the other hand, these results further confirmed that the aggregation of QDs could cause their RTP quenching. Finally, the 10 mM HEPES (pH 7.4) buffer without salt was selected in this work.

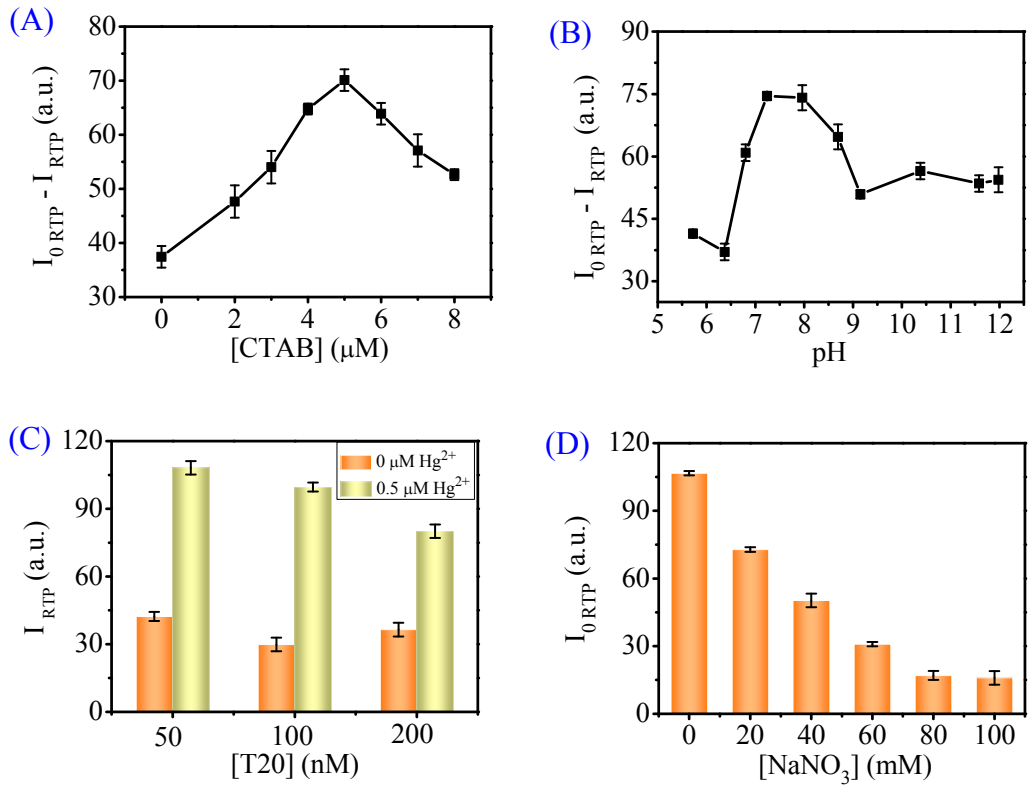


**Figure S2** (A) Effect of CTAB concentration on the quenching of RTP intensity of the T20/CTAB/Mn-ZnS (T20: 100 nM, Mn-ZnS: 0.15 mg/mL) in the presence of 500 nM $Hg^{2+}$; (B) Effect of pH on the quenching of RTP intensity of the T20/CTAB/Mn-ZnS (T20: 100 nM, CTAB: 5 μM, Mn-ZnS: 0.15 mg/mL) in the presence of 500 nM $Hg^{2+}$; (C) Effect of T20 concentration on the RTP intensity of CTAB/Mn-ZnS in the absence and presence of $Hg^{2+}$ (CTAB: 5 μM, Mn-ZnS: 0.15 mg/mL). (D) Effect of ionic strength on the phosphorescence emission of the CTAB/Mn-ZnS (CTAB: 5 μM, Mn-ZnS: 0.15 mg/mL). Here, $I_0$ and I represent the RTP intensities of QDs in the absence and presence of 500 nM $Hg^{2+}$, respectively; $\lambda_{ex}$ = 316 nm and the RTP intensities were recorded at 595 nm.

## 4. Fluorescence spectra of the T20/CTAB/Mn-ZnS with different concentrations of $Hg^{2+}$

As shown in Figure S3, the fluorescence intensity (emission wavelength at 600 nm) decreased with increasing $Hg^{2+}$ concentration. However, the second-order scattering (emission wavelength at 632 nm) strongly interferes with the fluorescence signals.

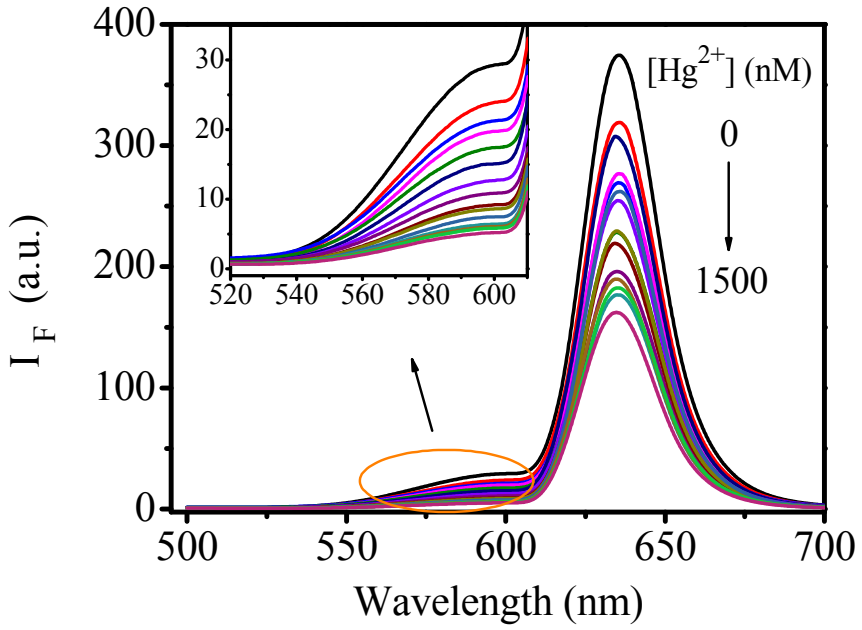


**Figure S3** Fluorescence spectra of the T20/CTAB/Mn-ZnS (100 nM/5 μM/ 0.15 mg/mL) in the presence of different concentrations of $Hg^{2+}$ ions (from top to bottom: 0, 50, 100, 200, 300, 400, 500, 600, 700, 800, 900, 1000, 1250, 1500 nM). The excitation wavelength was at 316 nm.

## 5. Comparison of this method for the detection of $Hg^{2+}$ with some other T-$Hg^{2+}$-T based methods.

**Table S1** Comparison of this method for the detection of $Hg^{2+}$ with other methods.

| Method | System | Linear range (nM) | Detection limit (nM) | Ref. |
|---|---|---|---|---|
| Electrochemistry | T-rich DNA/AuNPs/$[Ru(NH_3)_6]^{3+}$ | – | 10 | [2] |
| | T-rich DNA/Fc [a]-tagged | 0.1 – 5000 | 0.06 | [3] |
| Colorimetry | T-rich DNA/AuNPs [b] | – | 500 | [4] |
| | T-mononucleotides/AuNPs | 200–6000 | 50 | [5] |
| | T-rich DNA/AuNPs | 0 – 5000 | 500 | [6] |
| Fluorophotometry | FAM [c] labeled T-rich DNA/AuNPs | 96 – 6400 | 40 | [7] |
| | FAM labeled T-rich DNA/SWNTs [d] | 50 – 8000 | 14.5 | [8] |
| | T-rich/$Ru(phen)_2(dppz)^{2+}$ | 5 – 600 | 5 | [9] |
| | T-rich/QDs [e]/AuNPs | 6 – 60 | 6 | [10] |
| Phosphorescence assay | T-rich/QDs | 50 – 800 | 1.5 | This method |

[a] Fc (ferrocene); [b] AuNPs (gold nanoparticles); [c] FAM (carboxyfluorescein); [d] SWNTs (single-walled carbon nanotubes);[e] QDs (quantum dots).

## 6. The results obtained for the phosphorescence determination of $Hg^{2+}$

For tap water, the sample was collected after discharging tap water for about 20 min and boiled for 5 min to remove chlorine. River water sample was obtained from Chia-ling River. The sample collected was first filtered through a 0.2 μM filter membrane to remove oils.

**Table S2.** Detection of $Hg^{2+}$ in tap water sample using the proposed method (n = 5)

| Sample | Background Content (nM) | Concentration | | Recovery (%) | RSD (%) |
|---|---|---|---|---|---|
| | | Added (nM) | Found (nM) | | |
| Tap water 1 | ND | 100 | 96 | 96 | 3 |
| Tap water 2 | ND | 200 | 204 | 102 | 3 |
| Tap water 3 | ND | 300 | 287 | 95.7 | 4 |
| Chia-ling River 1 | ND | 100 | 112 | 112 | 3 |
| Chia-ling River 2 | ND | 200 | 216 | 108 | 3 |
| Chia-ling River 3 | ND | 300 | 318 | 106 | 2 |

ND: not detected

## References

[1] Y. He, H. F. Wang and X. P. Yan, *Anal. Chem.*, 2008, **80**, 3832;

[2] P. Miao, L. Liu, Y. Li and G. Li, *Electrochem. Commun.*, 2009, **11**, 1904;

[3] D. Wu, Q. Zhang, X. Chu, H. Wang, G. Shen and R. Yu, *Biosens. Bioelectron.*, 2010, **25**, 1025;

[4] N. Kanayama, T. Takarada and M. Maeda, *Chem. Commun.*, 2011, **47**, 2077;

[5] Y. Xu, L. Deng, H. Wang, X. Ouyang, J. Zheng, J. Li and R. Yang, *Chem. Commun.*, 2011, **47**, 6039;

[6] X. Xu, J.Wang, K. Jiao and X. Yang, *Biosens. Bioelectron.*, 2009, **24**, 3153.

[7] H. Wang, Y. Wang, J. Jin and R. Yang, *Anal. Chem.*, 2008, **80**, 9021;

[8] L. Zhang, T. Li, B. Li, J. Li and E. Wang, *Chem. Commun.*, 2010, **46**, 1476;

[9] B. N. Oh, S. Park, J. Ren, Y. J. Jang, S. K. Kim and J. Kim, *Dalton Trans.*, 2011, **40**, 6494;

[10] M. Li, Q. Wang, X. Shi, L. A. Hornak and N. Wu, *Anal. Chem.*, 2011, **83**, 7061.